Research Article

Chemical Review and Letters
journal homepage: www.chemrevlett.com
ISSN (online): 2645-4947 (print) 2676-7279

Role of manganese ion in tuning the structural and optical properties of silver sulfide nanostructures

Afrah Ahmed[1], Aula M. Al Hindawi[1], Nagham M. Shiltagh[2, *]

[1]*Department of Chemistry, College of Education for Pure Science, University of Kerbala, Karbala, Iraq*
[2]*Department of Physics, College of Science, University of Kerbala, Karbala, Iraq*

ARTICLE INFO

Article history:
Received 25 June 2024
Received in revised form 15 July 2024
Accepted 20 July 2024
Available online 20 July 2024

Keywords:
Ag_2S nanoparticles,
Mn-doped Ag_2S nanoparticles,
Optical properties.

ABSTRACT

Undoped and Mn-doped Ag_2S nanoparticles were prepared using the chemical precipitation method. The effect of the Mn ion on both the structural and optical properties of Ag_2S was investigated. The XRD pattern shows that Ag_2S particles are crystalline with a monoclinic phase. Doping Mn^{+2} into Ag_2S particles effects the crystalline structure and shifts the XRD peaks towards a longer diffraction angle. Debye-Schrrer's formula was used to estimate the crystalline size of undoped Ag_2S particles, and it was found to be 64.22 nm; however, the size was reduced after introducing Mn ions. FE-SEM images show that there is no effect of increasing dopant concentration on the particle shape and the majority are spherical. The optical properties of Ag_2S show a significant enhancement after doping with Mn ions, and the enhancement increases as the Mn concentration increases. The band gap energy of undopped and (10%)Mn-doped Ag_2S nanoparticles were estimated from their UV-Vis spectra and they are 3.87 eV and 3.93 eV, respectively.

1. Introduction

Developing and innovation thermoelectric and photovoltaic devices, which convert waste heat and solar light to electrical energy, respectively, have grabbed researchers' attention. These devices have the drawback that their efficiency of energy conversion is low because their semiconductor components have a narrow band gap. Moreover, the activities of some semiconductors, such as photocatalytic activity is limited due to their narrow band gaps [1, 2]. Therefore, many efforts to enhance the device's efficiency and improve its photocatalytic activity are reported. Doping and controlling the band gap energy are considered effective approaches to enhance the energy conversion efficiency [3]. Very recently, Arif Dar et al. developed electrodes for supercapacitor devices by doping SnSe material with Fe. The Fe-doped SnSe electrode exhibited high capacitance retention compared to undoped SnSe electrode [4]. Shim group performed an experiment where Ni atoms were added to SnS to form life-lasting electrodes for optoelectronic devices. It was found that Ni—doped SnS particles have flower-like shapes, and their size increases as the dopant concentration increases [5].

Metal chalcogenides have potential properties and can be used in fields such as solar cells, magnetic field sensors, supercapacitors, and superconductors [6-9]. Among metal chalcogenides, Ag_2S has been extensively studied because of their incredible properties. Ag_2S is an n-type semiconductor with a narrow band gap (0.9-1.05 eV) that emits light in the near infrared region (NIR), therefore, it was used for imaging the biological tissues because of its ability to penetrate tissues deeply without being absorbed and scattered by the tissues [10]. Nanoparticles play main role in the chemistry and physics fields [11b-f] such as the Ag_2S nanoparticles exhibit ultralow solubility product constants (Ksp= 6.3 × 10−50), meaning the biological systems do not release Ag ions. So, these properties pave the way to use these

∗ Corresponding author; e-mail: aula.m@uokerbala.edu.iq
https://doi.org/10.22034/crl.2024.464779.1365

NIR particles in biology and biomedicine applications [11a].

However, their small band gap restricts their applications in electronic and optoelectronic devices. Doping with transition metal ions could increase the charge separation and increase the band gap, and further their applications in fields like photocatalytic. Recent work by Liang's team has shown that the electrical performance of silver sulfide can be enhanced successfully by doping with transition metal ions, especially when the electrical conductivity increases by more than five orders of magnitude compared to the pure Ag_2S sample [12]. Additional enhancements to the properties of Ag_2S nanoparticles were reported by the Kang team. They observed that the absorption and emission of Ag_2S nanoparticles can be improved by doping them with Li ions and also enhance the NIR photoluminescence [13]. Many techniques have been proposed and used to form pure Ag_2S and doped Ag_2S nanoparticles, some of which are sonochemical [14] co-precipitation [15], green synthesis [16], sol gel [17] and hydrothermal methods with photoassisted deposition for doping metals into Ag_2S particles.[18] Jeong et al. have prepared both undoped and Mn- doped Ag_2S nanoparticles through co-pyrolysis of Ag and Mn single source precursors using silver diethyldithiocarbamate and manganese

bis(diethyldithiocarbamate) as starting materials [19]. They found that Mn ions have a negligible effect on the crystal structure of Ag_2S particles, however, doping Ag_2S with Mn reduced the photoluminescent intensity. As well as, manganese incorporated Ag_2S was prepared using 3-mercaptopropionic acid as a growth template. The authors found that Mn plays a vital role in enhancing the optical and electrical properties of Ag_2S [20]. The Hota group successfully doped the Mn ion into Ag_2S crystal lattice using a temperature-controlled refluxing technique. They found that Mn-doped Ag_2S nanoparticles exhibit great electrocatalytic activity for hydrogen evaluation reaction [21].

In this paper, one of the key objectives was to demonstrate the doping process to see whether this allows access to particles with larger band gap than observed without dopants. This study therefor involved the addition of a transition metal ion (Mn+2) to the starting materials, which will hopefully reduce the aggregation of particles and form small particles with wide band gap. These may have a number of uses including optical applications where the scattering of light plays a role in enhancing signals.

2. Computational details

2.1. Chemicals

Sliver acetate (99.9%, CH_3CO_2Ag) and sodium sulfide (99%, Na_2S) were purchased from THOMAS BAKER, India. Manganese sulphate ($MnSO_4.H_2O$) 99% was purchased from QualiKems Fine Chem.

2.2. Preparation of silver sulfide

To prepare silver sulfide nanoparticles, initially 0.167 g of silver acetate (0.01 M) was dissolved in 100 mL of deionized water and stirred until no visible particles were seen.

Sodium sulfide solution was prepared by dissolving 0.078 g of Na2S (0.01 M) in 100 mL deionized water and then adding dropwise into silver acetate solution. After completing the addition, the solution was left on the magnetic stirrer for one hour at 50 ^oC (the optimal conditions for producing doped and undoped Ag_2S nanoparticles). Finally, the precipitated was collected and dried for 3 hours at 50 ^oC after centrifugation at 4000 rpm. Different concentrations of Mn-doped Ag_2S solutions were prepared (2%, 4%, 6% 8%, and 10 wt.%) by adding the proper amount of ($MnSO_4.H_2O$) to silver acetate solution before adding sodium sulfide solution.

2.3. Characterization and instrumentations

To characterize the as-prepared silver sulfide nanoparticles, many techniques were utilized. X-ray diffraction (X pert pro-PANalytical company) was used to study the crystalline structure of Ag_2S sample. The size and morphology of both Mn-doped and undoped particles were determined using field emission scanning electron microscope (FE-SEM), which was equipped with EDX to provide information about the elemental composition of the samples. FTIR (IRAffinity-1S, SHIMADZU) was used to confirm the formation of the Ag-S bond and to study the functional groups. The optical properties of the prepared nanoparticles were examined using UV-Vis spectrometer (UV-1800 Shimadzu spectrophotometer, Japan).

3. Results and Discussion

After mixing the precursors, the color of the solution changed from colorless to gray-blackish solution which is attributed to the formation of Ag_2S nanoparticles. Direct evidence for the incorporating Mn ions into Ag_2S nanoparticles has been presented through studies of the crystalline structures of both undoped and Mn-doped Ag_2S. As can be seen from Figure 1 the diffraction peaks for both pure Ag_2S and Mn-doped Ag_2S nanoparticles are consistent with monoclinic Ag_2S according to JCPDS

Card no. 14-0072. The diffraction peaks are positioned at bragg's angle 26.32º, 28.97º, 31.51º, 33.62º, 34.39º, 36.82º, 37.73º, 40.75º, 43.40º, 45.44º, 46.20º, 47.77º, 48.76º, 53.27º, 58.36º, and 63.75º correspond to the X-ray diffraction from planes -101, 111, -112, 120, -121, 121, -103, 031, 200, 023, 113, 311, 212, 222, 024 and 034, respectively [22]. Doping Ag_2S nanocrystals with transition metal ions leads to a decrease in the intensity of diffraction peaks, and the decrease becomes more obvious as the concentration of Mn increases, which is quite similar to the previous work when the researchers doped Ag_2S particles with Pb ions [23]. The appearance of several broadened peaks in the XRD pattern after doping is attributed to the presence of Mn ions, which may induce defects into Ag_2S crystal lattice [24]. It is clear from the expanding XRD patterns (Figure 1(b)) that the Mn ion has an effect on the crystalline structure of Ag_2S. A notable shift in the diffraction peaks of Mn-doped Ag_2S towards a longer angle compared with pure Ag_2S can be seen, which could be attributed to the incorporation of the Mn ion into the Ag_2S crystal structure, leading to a change in the lattice parameters of Ag_2S particles. Furthermore, it was known that the ionic radii of both the doped ion and the base metal have a great effect on the diffraction peaks of the XRD pattern and may cause lattice distortion, which would change the interatomic distances and, consequently, the locations of the XRD peaks. Hence, the lattice parameters of silver sulfide become smaller after doping with Mn ion because the substitution of a larger ion (the ionic radius of Ag ion is 1.15 Aº) [25] by a smaller ion (the ionic radius of Mn+2 = 0.67 Å) may lead to contraction in the lattice fringe distance and then increasethe diffraction angle (2θ) [26, 27]. Thus, XRD pattern analysis is essential for characterizing the crystal structure of undoped and Mn-doped Ag_2S nanoparticles, which provides detailed information about crystallographic parameters, particle size, and the structural effects of doping, leading to understanding and optimizing the material's properties for different applications.

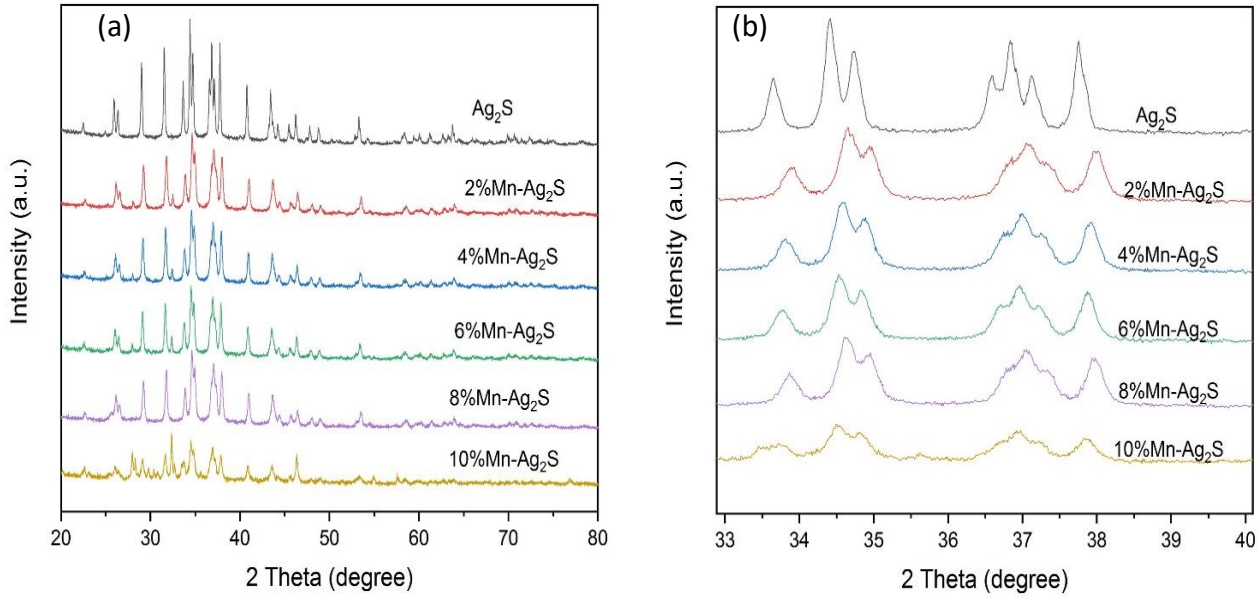

Fig. 1. XRD pattern for un-doped and Mn-doped Ag_2S nanoparticles using different concentrations of Mn ion (a) and expanded view of XRD curved between 33º and 40º (b).

The crystallite size for undoped and doped Ag_2S particles was obtained from the Scherrer equation [28] using the high intensity peaks at a diffraction angle of 34.39º.

$D = K\lambda/\beta\cos\theta$ ……. (1)

Here the wavelength of the Cukα is 0.15406, θ is the diffraction angle, k is a constant equal to 0.9, and β is the full width at a half maximum. The crystallite size is represented in Table (1) and there is a decrease in the size of the crystallite as the concentration of Mn ions increases, this observation can be attributed to the inhibition of the growth of crystallites by metal doping [29].

Table 1. Crystallite sizes of Mn-doped and undoped Ag_2S nanocrystals obtained from XRD patterns.

Dopant concentrations	Diffraction angle (deg.)	FMHW (nm)	Crystallite size (nm)
10%	34.4873	0.2764	30.09467
8%	34.6067	0.2368	35.13878
6%	34.5117	0.2285	36.40576
4%	34.551	0.2254	36.9104
2%	34.6173	0.1499	55.51103
un-doped Ag_2S	34.392	0.1296	64.22356

FTIR spectra for pure Ag_2S and Mn-doped Ag_2S nanoparticles were recorded in the range of 400 -4000 cm-1 as shown in Figure 2. The peaks that appear in the region between 400 -600 cm-1 are assigned to the Ag-S bond, conforming to the formation of silver sulfide nanoparticles [24]. The major difference between the spectra of undoped and Mn-doped Ag_2S nanoparticles is the appearance of a strong band at 1119 cm-1 in the spectrum of Mn-doped, which could be attributed to the formation of Ag-S-Mn. This finding is quite similar to the spectrum of doping Mn into ZnS nanoparticles [30]. The best explanation for this peak is the result of the substitution of the Mn ion into the Ag_2S lattice.

The effect of doping Mn ions into Ag_2S particles on their surface morphology was studied using the FE-SEM technique. Images in Figure 3 show that all the particles are nearly spherical in shape, meaning Mn ions have a negligible effect on the shape of the hosted Ag_2S particles, and this observation is in good agreement with the XRD results. The Mn ion has an effect on the size of Ag_2S nanoparticles (the average diameter is found to be in the range of 35.1 nm (10% Mn) to 64.3 nm (0% Mn)). This decrease in their size after incorporating Mn ions could be related to the substitution of a large silver ion with a small Mn ion, leading to a contraction in their size.

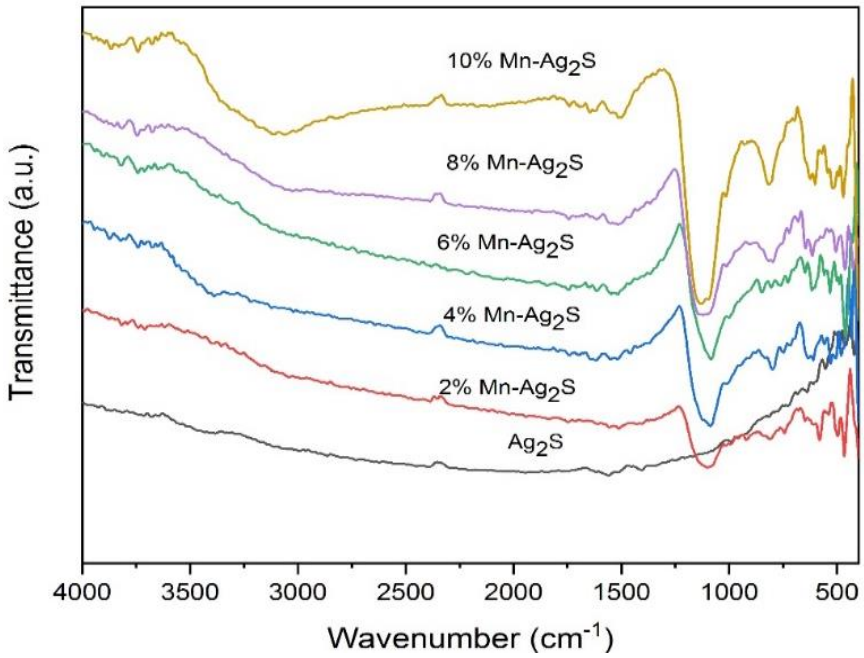

Fig. 2: FTIR spectra for undoped and Mn-doped AgS nanoparticles.

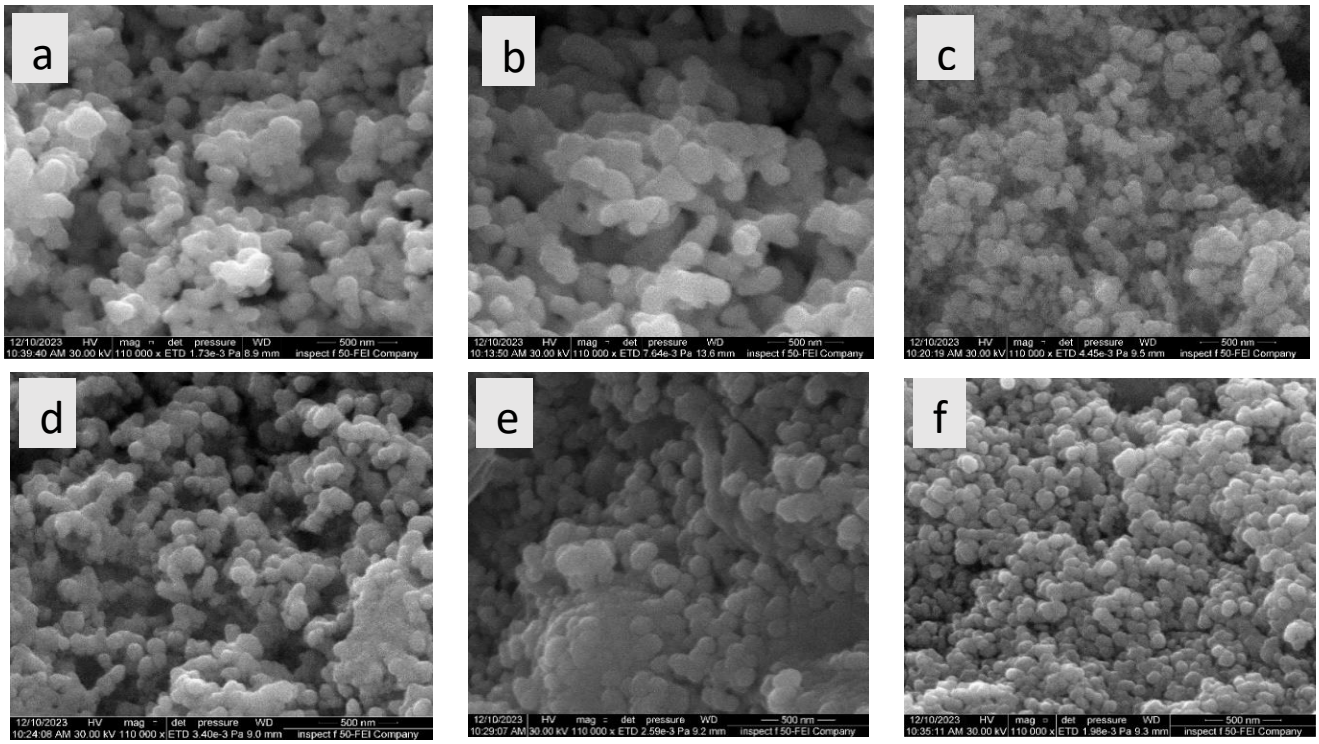

Fig. 3. FE-SEM images for undoped and Mn-doped Ag_2S nanoparticles, (a) un-doped particles, (b) 2%, (c) 4%,(d) 6%, (e) 8%, and (f) 10%. The scale bar for all images is 500 nm.

The EDS chart, which is presented in Figure 4(a), shows the appearance of only silver and sulfide elements in the prepared particles. However, samples doped with different concentrations of Mn ions showed an additional peak referring to the presence of Mn ions in the samples (Figure 4(b) shows the EDS chart for only 10% Mn-doped Ag_2S particles, and the inset shows the atomic and weight percentages for each element). Although the EDS chart cannot determine the exact position of Mn ions in the crystalline structure of Ag_2S, it confirms the presence of manganese in Ag_2S particles by detecting characteristic X-ray emissions at particular energies related to manganese and comparing these emissions to known standards.

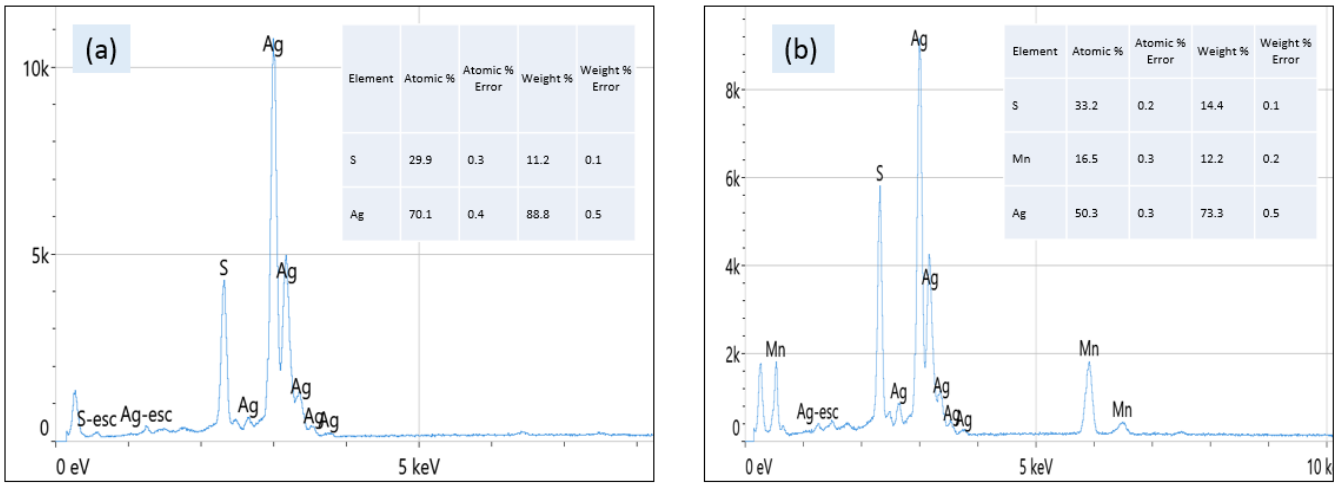

Fig. 4. EDS charts for (a) undoped Ag_2S particles and (b) 10% Mn-doped Ag_2S nanocrystalles. The insets represent the atomic and wieght percentage for each elecment in the sample.

A strong enhancement in the absorption intensity of Mn-doped Ag_2S nanoparticles can be observed compared to the undoped-Ag_2S nanoparticles spectrum presented in Figure 5(a), indicating an enhancement in the optical properties of Ag_2S nanoparticles after doping Ag_2S particles with Mn ions. This absorption enhancement leads to improvements in photocatalytic activity of semiconductor, in addition to the efficiency of energy conversion [31]. The exponential decline in the absorption curve tail can be used to determine the absorption edge and is found to be around 600 nm. The band gap energy for all the prepared samples was calculated using Tauc equation and the value was estimated from the extrapolation of the linear part of UV-Visible curve [32-34]. Generally, the band gap energies of undoped and Mn-doped Ag_2S nanoparticles are larger than that of bulk Ag_2S (0.9-1.05 eV) [35]. It seems from Figure 5(b) that as the concentration of Mn ion increases the band gap energy increases (Eg~ 3.90 eV, 3.885 eV, 3.91 eV, 3.89 eV, and 3.93 eV at 2%, 4%, 6%, 8%, and 10%, respectively) compared with undoped particles (Eg~ 3.87 eV). The reason for this increment could be related to the Mn ions, which produce significant modifications in the energy levels of host particles. In other words, the "charge transfer" transition from Mn d-orbital to the conduction band of Ag_2S is responsible for tuning band gap energy. As a result, by altering the doping concentration one can be able to tuning the band gap energy according to the desired applications.

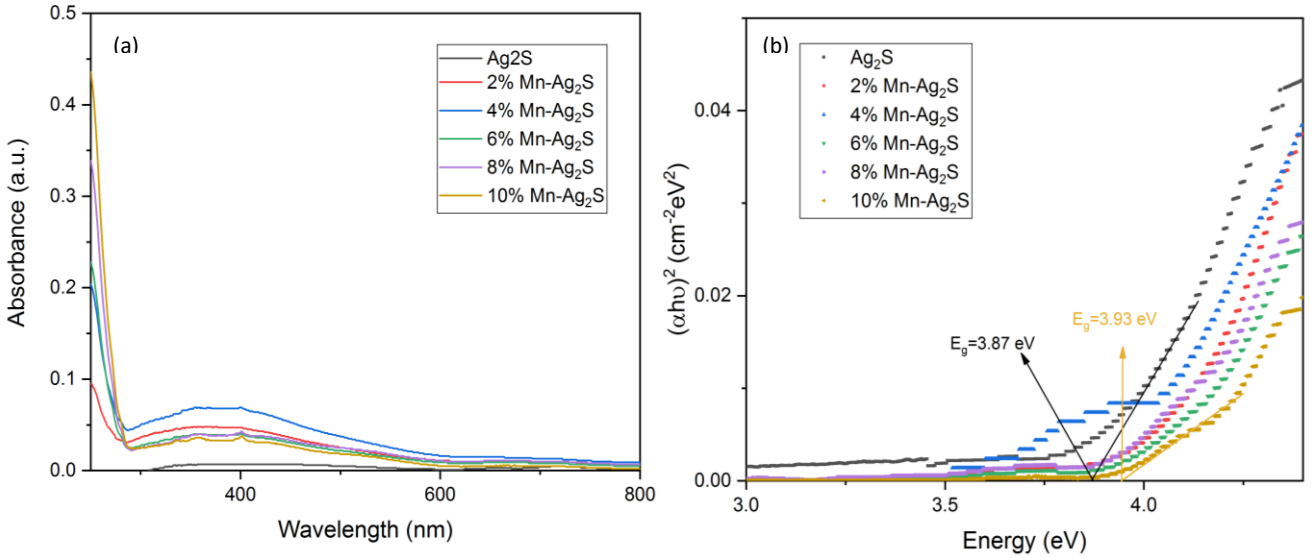

Fig. 5. UV-Vis absorption spectra for silver sulfide nanoparticles (a) and band gap energies of undoped and doped Ag_2S nanoparticles (b).

4. Conclusion

Doping narrow band gap semiconductor nanoparticles with transition metal ions is considered a stepping stone for improving their optical and structural properties. In this work, silver sulfide nanoparticles were doped with Mn ion to study the effect of doping on their properties. Both undoped and doped nanoparticles were characterized using different techniques: FE-SEM, EDS, XRD, FTIR and UV-Visible spectroscopy. The findings show that increasing the concentration of the metal ions leads to a shift in XRD peaks towards a longer diffraction angle compared with undoped Ag_2S, suggesting the substitution of a larger ion (Ag) by Mn ion. FE-SEM images show that there is no effect of increasing dopant concentration on the particle shape and the majority are spherical. An improvement in the absorption of Ag_2S nanoparticles was observed after the addition of Mn ion. The doped particles have a larger band gap (~3.93 eV) respect to the pure particles. A significant peak (1119 cm-1) was observed in the FTIR spectrum of doped particles, which is related to Ag-S-Mn bond, confirming the doping process.

Acknowledgments

The authors would like to thank the Department of Chemistry, College of Education for Pure Science, University of Kerbala and Department of Physics, College of Science, University of Kerbala, for supporting this work.

Declaration of Competing Interest

The authors declare that they have no known competing financial interests or personal relationships that could have appeared to influence the work reported in this paper.

Data availability

No data was used for the research described in the article.

References

[1] A. Q. Abed, A. M. A. Hindawi, and H. F. Alesary, "Synthesis and characterization of zinc sulfide nanomaterials for removal methylene blue dye from aqueous solution," in AIP Conference Proceedings, (2023).

[2] N. M. Shiltagh, N. J. Ridha, A. M. A. Hindawi, K. J. Tahir, R. A. Madlol, H. F. Alesary, et al., "Studying the optical properties of silver nitrates using a pulsed laser deposition technique," in AIP Conference Proceedings, (2020).

[3] H. N. Nam, R. Yamada, H. Okumura, T. Q. Nguyen, K. Suzuki, H. Shinya, et al., "Correction: Intrinsic defect formation and the effect of transition metal doping on transport properties in a ductile thermoelectric material α-Ag 2 S: a first-principles study," Physical Chemistry Chemical Physics, 23 (2021) 8938-8938.

[4] M. A. Dar, S. Majid, M. Satgunam, K. M. Batoo, S. Kalpana, P. Arularasan, et al., "Electrochemical performance of Fe-doped SnSe material electrodes for supercapacitors," Journal of Energy Storage, 94 (2024) 112403.

[5] M. A. Dar, S. Dinagaran, K. M. Batoo, S. R. Ahamed, S. Hussain, Z. Ahmad, et al., "Morphological nanoflowers of Ni-doped SnS for high-performance electrode materials for supercapacitors," Journal of Energy Storage, 68, (2023) 107717.

[6] R. R. G. Martínez, C. A. R. González, J. F. HernándezPaz, F. J. Vega, H. C. Montes, and I. O. Armendáriz, "Synthesis and Characterization of Carbon Aerogels Electrodes Modified by Ag 2 S Nanoparticles," Materials Research, 24 (2021).

[7] J. Amaya Suárez, C. García-Prieto, M. D. FernándezMartínez, E. R. Remesal, A. M. Márquez, and J. Fernández Sanz, "Optoelectronic properties of Ag2S/graphene and FeS2/graphene nanostructures and interfaces: A density functional study including dispersion forces," Journal of Materials Research, 37 (2022) 1047-1058.

[8] I. Manohara Babu and I. Rathinamala, "Silver sulfide nanosheets: a proficient electrode material for energy storage," Ionics, 29 (2023)4617-4627.

[9] G. Topcu, A. M. Al Hindawi, C. Feng, D. Spence, B. Sitorus, H. Liu, et al., "Precision engineering of nanoassemblies in superfluid helium by the use of van der Waals forces," Communications Chemistry, 7 (2024) 125.

[10] Y. Cai, Z. Wei, C. Song, C. Tang, W. Han, and X. Dong, "Optical nano-agents in the second near-infrared window for biomedical applications," Chemical Society Reviews, 48 (2019) 22-37.

[11] (a) C. Ding, Y. Huang, Z. Shen, and X. Chen, "Synthesis and bioapplications of Ag_2S quantum dots with nearinfrared fluorescence," Advanced Materials, 33 (2021) 2007768; (b) F. Arjomandi Rad, J. Talat Mehrabad, E. Dargahi Maleki, Synthesis and characterization of Gabapentin-Zn2 Al-LDH nanohybrid and investigation of its drug release and biocompatibility properties on a laboratory scale, J. Chem. Lett. 5 (2024). 10.22034/jchemlett.2024.442139.1157; (c) A. K. O. Aldulaim, N. M. Hameed, T. A. Hamza, A. S. Abed, The antibacterial characteristics of fluorescent carbon nanoparticles modified silicone denture soft liner. J. Nanostruct., 12 (2022) 774-781. doi:10.22052/JNS.2022.04.001; (d) P. O. Ameh, Removal of Methylene Blue from Aqueous Solution using Nano Metal Oxide Prepared from Local Nigerian Hen Egg Shell: DFT And Experimental Study, *Chem. Rev. Lett.* 6 (2023) 29-43. 10.22034/crl.2023.328721.1155; (e) E. Vessally, M.R. Ilghami, M. Abbasian, Investigation the Capability of Doped Graphene Nanostructure in Magnesium and Barium Batteries with Quantum Calculations, Chem. Res. Technol. 1 (2024). 10.2234/chemrestec.2024.436837.1007; (f) B. Baghernejad, F. Nuhi, A new approach to the facile synthesis of 1,8-dioxooctahydroxanthene using nano-TiO2/ CNT as an efficient catalyst, *Chem. Rev. Lett.* 6 (2022) 268-277. 10.22034/crl.2022.340828.1166; (g) P. O. Ameh, Synthesized iron oxide nanoparticles from Acacia nilotica leaves for the sequestration of some heavy metal ions in aqueous solutions, *J. Chem. Lett.* 4 (2023) 38-51. 10.22034/jchemlett.2023.360137.1083; (h) H. Ashassi-Sorkhabi, A. Kazempour, J. Mostafaei, E. Asghari, Impact of ultrasound frequency on the corrosion resistance of electroless nickel-phosphorus-nanodiamond plating, *Chem. Rev. Lett.* 6 (2022) 187-192. 10.22034/crl.2022.345098.1169; (i) Milad. Sheydaei, M. Edraki, Poly(butylene trisulfide)/CNT nanocomposites: synthesis and effect of CNT content on thermal properties, *J. Chem. Lett.* 3 (2022) 159-163. 10.22034/jchemlett.2023.380990.1101; (j) T.G. Naghiyev. Neutron-alpha reactions in nano α-Si_3N_4 particles by neutrons. *Modern Physics Letters A* **36**(24) (2021) 2150181. https://doi.org/10.1142/S0217732321501819;

[12] J. Liang, T. Wang, P. Qiu, S. Yang, C. Ming, H. Chen, et al., "Flexible thermoelectrics: from silver chalcogenides to full-inorganic devices," Energy & Environmental Science, 12 (2019) 2983-2990.

[13] M. H. Kang, S. H. Kim, S. Jang, J. E. Lim, H. Chang, K.-j. Kong, et al., "Synthesis of silver sulfide nanoparticles

and their photodetector applications," RSC advances, 8 (2018)28447-28452.

[14] M. Geravand and F. Jamali-Sheini, "Synthesis and physical properties of un-and Zn-doped Ag2S nanoparticles," Advanced Powder Technology, 30(2019) 347-358.

[15] S. Sharath, D. Gayathri, S. R. Mannopantar, and M. Kalasad, "Growth and characterization of Ag2S semiconductor nanoparticles," Materials Today: Proceedings, 67(2022) 276-279, 2022.

[16] A. M. AL HINDAWI, N. H. OBAID, I. JOUDAH, N. SHILTAGH, and K. TAHIR, "Fabrication and Characterization of Silver Nanoparticles Using Plant Extract," International Journal of Pharmaceutical Research (09752366) 12(2020).

[17] S. V. Singh, U. Gupta, B. Mukherjee, and B. N. Pal, "Role of electronically coupled in situ grown silver sulfides (Ag2S) nanoparticles with TiO2 for the efficient photoelectrochemical H2 evolution," International Journal of Hydrogen Energy, 45(2020) 30153-30164.

[18] E. O. Ichipi, S. M. Tichapondwa, and E. M. Chirwa, "Plasmonic effect and bandgap tailoring of Ag/Ag2S doped on ZnO nanocomposites for enhanced visiblelight photocatalysis," Advanced Powder Technology, 33 (2022)103596.

[19] S. Jeong, H. Doh, and S. Kim, "Colloidal Second NearInfrared-Emitting Mn-Doped Ag2S Quantum Dots," ChemNanoMat, 6(2020)538-541.

[20] F.-F. Wu, Y. Zhou, J.-X. Wang, Y. Zhuo, R. Yuan, and Y.-Q. Chai, "A novel electrochemiluminescence immunosensor based on Mn doped Ag2S quantum dots probe for laminin detection," Sensors and Actuators B: Chemical, 243(2017) 1067-1074.

[21] P. Hota, S. Bose, D. Dinda, P. Das, U. K. Ghorai, S. Bag, et al., "Nickel-doped silver sulfide: An efficient air-stable electrocatalyst for hydrogen evolution from neutral water," ACS omega, 3(2018)17070-17076.

[22] M. S. Hamed, M. A. Adedeji, Y. Zhang, and G. T. Mola, "Silver sulphide nano-particles enhanced photo-current in polymer solar cells," Applied Physics A, 126(2020) 207.

[23] Y. Shu, J. Yan, Q. Lu, Z. Ji, D. Jin, Q. Xu, et al., "Pb ions enhanced fluorescence of Ag2S QDs with tunable emission in the NIR-II window: Facile one pot synthesis and their application in NIR-II fluorescent bio-sensing," Sensors and Actuators B: Chemical, 307(2020) 127593.

[24] P. Torabi and M. Moradian, "Preparation of Ag2S Nanoparticles and using as Catalyst for the A3-coupling (Aldehyde-Amine-Alkyne) Reaction," Journal of Nanostructures, 9 (2019)478-488.

[25] T. Gurgenc, "Structural characterization and dielectrical properties of Ag-doped nano-strontium apatite particles produced by hydrothermal method," Journal of Molecular Structure, 1223(2021) 128990.

[26] J. Tie, G. Xu, Y. Li, X. Fan, Q. Yang, and B. Nan, "Study on Enhancing the Thermoelectric Stability of the β-Cu2Se Phase by Mn Doping," Materials, 16 (2023) 5204.

[27] A. K. De, S. Majumdar, S. Pal, S. Kumar, and I. Sinha, "Zn doping induced band gap widening of Ag2O nanoparticles," Journal of Alloys and Compounds, 832 (2020)154127.

[28] A. Abed, A. Al Hindawi, and H. Alesary, "Green synthesis of zinc sulfide nanoparticles for the removal of methylene blue dye from aqueous solution," Nano World J, 8(2022) 79-84.

[29] K. Raja, P. Ramesh, and D. Geetha, "Structural, FTIR and photoluminescence studies of Fe doped ZnO nanopowder by co-precipitation method," Spectrochimica acta part A: molecular and biomolecular spectroscopy, 131(2014)183-188.

[30] K. Sharma, P. Kumar, G. Verma, and A. Kumar, "Optical properties of transition metal doped ZnS nanoparticles in PVK based nanocomposite films," Optik, 206(2020) 164357, 2020.

[31] N. Sun, X. Si, L. He, J. Zhang, and Y. Sun, "Strategies for enhancing the photocatalytic activity of semiconductors," International Journal of Hydrogen Energy, 58(2024) 1249-1265.

[32] Z. Turki, A. Al Hindawi, and N. Shiltagh, "Green Synthesis of CdS Nanoparticles Using Avocado Peel Extract," NanoWorld J, 8(2022) 73-78.

[33] A. M. Al Hindawi, I. Joudah, S. Hamzah, and Z. Tarek, "Plant extract: safe way for fabrication silver nanoparticles," in IOP Conference Series: Materials Science and Engineering, 2019 (2019) 012069.

[34] Z. T. Turki, A. M. A. Hindawi, and N. M. Shiltagh, "Fabrication and characterization of cadmium sulfide nanoparticles using chemical precipitation method," AIP Conference Proceedings, 2834 (2023).

[35] M. Hraja, A. Al Hindawi, and N. Shiltagh, "Investigation of Electronic and Molecular Features of Zn3S3/PEG4000 Nano-Composite Using the DFT Method," Journal of the Turkish Chemical Society Section A: Chemistry, 11(2024) 565-574.